IEEE Access
Multidisciplinary ⋮ Rapid Review ⋮ Open Access Journal

Received 18 February 2024, accepted 7 March 2024, date of publication 13 March 2024, date of current version 21 March 2024.

Digital Object Identifier 10.1109/ACCESS.2024.3376645

RESEARCH ARTICLE

Fixed-Wing UAV Formation Robust Fault-Tolerant Control With Switching Topologies

JINLIN LI[1,2], FEI GUO[1], AND JUNMIN ZHAO[2]
[1]Department of Mechanical Engineering, Tsinghua University, Beijing 100084, China
[2]Xi'an Modern Control Technology Research Institute, Xi'an 710065, China

Corresponding author: Fei Guo (guof2014@mail.tsinghua.edu.cn)

This work was funded by the Key Basic Research Program for Base Strengthening Project of China (2020-JCJQ-ZD-076-00).

ABSTRACT Motivated by the demand for formation security, this paper studies the fault-tolerant control problem for fixed-wing UAV formation with switching topologies. Based on the application of fixed-wing UAV formation in scenarios involving various severities of faults, this article employs a leader-follower formation control method, focusing on addressing actuator faults, saturation, failures and the consequent communication faults. These challenges are approached as a problem of fault-tolerant control with switching topologies. To tackle these problems, the article delves into the impact of UAV network connections on nodes through neighboring interactions and proposes a novel fault-tolerant formation control method based on graph theory, observer theory, output regulation, and H_∞ robust control theory, which is concluded as an algorithm. The method aims to effectively manage the complexities arising from fault occurrences and ensure the formation cooperative performance. Finally, the proposed control method's effectiveness is demonstrated in a formation with one leader and four followers through numerical simulations, with a comparative analysis against an alternative method. A formation security schema is developed to provide an application scenario of the proposed method for different kinds of fixed-wing UAV formations.

INDEX TERMS Fixed-wing UAV, leader-follower formation control, fault-tolerant control, switching topologies.

I. INTRODUCTION

In recent decades, unmanned aerial vehicle (UAV) plays a very important role in field of military, agriculture, industry and so on. In order to further take advantage of UAV, communication technology was used to create formation. Although quadrotor UAVs are more commonly used in general experimental situations [1], fixed-wing ones have more important applications in scenarios with large range and high altitude [2]. Compared to single UAV, control methods are more complex and challenging to be developed. One important part in application is formation security with accidents. A meaningful scenario in practice is that UAVs in the formation happen to have actuator faults and even crash in severe cases and later new UAV would replace the failing one, reconfiguring the network between UAVs, which can also happen with communication faults [3]. In such a practical situation for formation security three main scientific problems can be summarized: UAV formation realization, fault-tolerant control and switching topologies. There are enormous state-of-the-art methods to handle the relevant problems.

Formation control methods are based on information of agents in the whole group, which can be divided into three parts: position-based control, displacement-based control and distance-based control [4]. In position-based control agents sense their own positions with respect to a global coordinate system and the displacement-based control utilizes relative positions of neighbors, while the distance-based control take information in local coordinate systems. The cost of method aforementioned increases with the increasing of sensing capabilities and interactions. In this paper, apart

The associate editor coordinating the review of this manuscript and approving it for publication was Yang Tang.

from the distance-based control method for fixed-wing UAV formations [5], displacement-based control method are used to make a trade-off between cost and sensing capabilities.

UAV formation is a part of multi-agent system and excellent researches of formation control have been proposed in the field of multi-agent system in a broad sense. There were distributed control methods like artificial potential field and virtual pipeline method for collision avoidance [6]. In general fixed-wing UAV formation application scenarios, distance between different UAVs were large enough to minimize the probability of collision, which means consensus leader-follower formation control is sufficient for most circumstances. Dong et al. [7] came up with necessary theories for UAV formation control. In [8], further time-varying formation control method for heterogeneous systems was proposed. However, the relationship between network and control still remained unknown, covering the influence of neighbors in formation. There are also interesting event-triggered control method proposed to reduce the cost of network, guaranteeing the performance of control of the whole system [9], [10].

Furthermore, there were plenty of researches on fault-tolerant control and network system control with communication topologies [11], [12]. Cao et al. [13] provided a leader-follower consensus control method with external disturbances. In [14] and [15], data-driven fault diagnosis methods were proposed for fixed-wing UAVs. In [16], multi-agent consensus control under actuator saturation was proposed, and in [17], fault observers anti-windup schemes were utilized against faults and saturation. Besides, in [18], asymmetric saturation was considered in path following of surface vessels and addressed by designing auxiliary systems in light of sight guidance law to adjust the state trajectory. Meanwhile [19] also proposed an adaptive Kalman filter for UAV sensor/actuator faults. To be specific, fault-tolerant methods can be classified into active ones [20] and passive ones [21]. Reference [22] came up with a fault-tolerant consensus method for multi-agent systems based on fault estimation observer, which can detect fault information simultaneously. To consider a more complex scenario, in [23], fault-tolerant control under actuator faults with H_∞/H_2 performance constraints were put forward. Xu and Wu [24] came up with an adaptive event-triggered fault-tolerant control for synchronization of the multi-agent systems where fault rates could be boundedly estimated by designed adaptive law. Zhang et al. [25] raises an active fault-tolerant control method for second-order multi-agent system. Zhang et al. [26] proposed an event-triggered adaptive fault-tolerant control method for fixed-wing UAVs, where communication topology was only used for navigation with relative information instead of consensus control. In [27], a fractional-order fault-tolerant coordinated control against faults and communication delays was proposed for practical situations. In [28], a fractional-order adaptive formation fault-tolerant formation control with prescribed performance was put forward, which provided enlightenment for formation security problems for more practical situations. Qin et al. [29] presented a formation-containment FTC method for fixed-wing UAV swarm against faults, which was the position-based and disturbance-observer-based control with compensation for faults.

As for network control with switching topologies, researches in [30] and [31] proposed an event-triggered control with switching topologies to lower the cost of network consumption. Reference [32] raised a formation tracking control for heterogeneous multi-agent system, taking both switching topologies and time-varying delays into consideration. In [33], second-order multi-agent system control method with switching directed topologies are proposed. In [34], intelligent method like deep reinforcement learning was leveraged in multi-agent systems with switching topologies. Reference [35] proposed a UAV loss detection and auto-replacement protocol which can be logically replace the UAV when faults or failures happened. References [36] and [37] proposed a formation output regulation method for heterogeneous system. However, systems with switching topologies were different from switching system because topologies mainly influence the inputs instead of the system itself, which means that the method to address the problem of communication remains challenging.

There are still a few researches to synthesize the fault-tolerant control and switching network topologies. Yang et al. [38] proposed a fault-tolerant cooperative control based on topology reconfiguration. However, reconfiguration was regarded as a way to change the control structure instead of network between UAVs. Miao et al. [39] recently developed a fault-tolerant control method with Markovian switching topologies, lacking the analysis of influence by topology structures. Wu et al. [40] proposed a time-varying formation fault-tolerant control, however more practical situations and analysis on the internet remains unexplored and challenging.

In conclusion, although the field has yielded numerous insights into multi-agent formation fault-tolerant control and switching topologies, a comprehensive integration with a focus on formation security remains relatively under-explored, defining the pivotal focus of this paper. Drawing inspiration from this analysis and motivated by demand for formation security, the paper amalgamates fault and failure scenarios, treating them as a unified challenge through fault-tolerant control with switching topologies for fixed-wing UAV formation. Besides, under the condition combined with actuator faults, saturation, failures and communication faults, some classic compensatory fault-tolerant control methods may not meet the requirements, especially when considering the cost of saturated UAV actuator and computational power constraints. Therefore, robust control

methods are preferred to achieve optimal performance control at a lower cost for a wide range of uses like small fixed-wing UAVs. The research therefore introduces a novel formation robust fault-tolerant control method with switching topologies, emphasizing the performance assurance of the entire formation through the novel application of the H_∞ method in such a challenging situation, which could be helpful to researchers with similar concerns like the formation security of some cost-constrained fixed-wing UAVs. The key contributions can be summarized as follows:

1) Building on the practical significance of real-world scenarios, the study uniquely considers the simultaneous presence of actuator faults and saturation, treating them as bounded additive faults. It develops an output regulation method for trajectory calculations using the Dubins path algorithm and incorporates a distributed observer (DO) for precise state estimation of followers within the composite system. These features collectively form the foundational framework of the study.
2) The study conducts an analysis of the leader-follower connected graph structure in formation consensus control, thereby enabling effective control of the entire formation system with switching topologies. Leveraging the structure of the Laplacian matrix, the study divides the formation consensus problem into more manageable separated ones, simplifying the design of control laws and uncovering the intricate influence of UAV networks on individual agents through neighboring interactions, through which an auxiliary system could be formed for formation fault-tolerant control. This analysis is consolidated in Theorem 1.
3) Based on a comprehensive examination of the fault and topology structure, the study develops a formation robust fault-tolerant control (FRFTC) framework under the H_∞ approach, ensuring the stabilization of UAV formations within fault-prone environments and switching topologies. The theorem 2 encapsulates the crucial findings from this analysis. The proposed method's effectiveness is further verified through simulation tests, including comparative evaluations with other existing methodologies.

The rest of this paper is organized as follows. Section II presents fundamental mathematical concepts, including model construction, linear output regulation, and graph theory. In Section III, the problem of fault-tolerant control with switching topology is addressed with the H_∞ method. Section IV provides a detailed numerical simulation to validate the proposed method. Finally, Section V offers a comprehensive conclusion of this work.

II. PRELIMINARIES

A. MODEL CONSTRUCTION

The model construction of a fixed-wing UAV consists of mainly seven parts From Fig. 1, which describes the

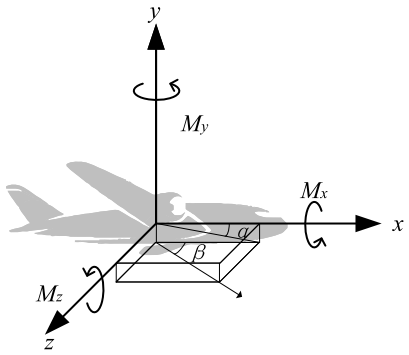

FIGURE 1. Model construction of a fixed-wing UAV.

movement of a fixed-wing UAV under control.

$$\begin{cases} m\dfrac{\mathrm{d}\boldsymbol{V}}{\mathrm{d}t} = \dfrac{\delta \boldsymbol{V}}{\delta t} + \boldsymbol{\Omega} \times \boldsymbol{V} = \boldsymbol{F} + \boldsymbol{P} \\ \dfrac{\mathrm{d}\boldsymbol{H}}{\mathrm{d}t} = \dfrac{\delta \boldsymbol{H}}{\delta t} + \boldsymbol{\omega} \times \boldsymbol{H} = \boldsymbol{M} + \boldsymbol{M}_P \\ \dfrac{\mathrm{d}\boldsymbol{X_p}}{\mathrm{d}t} = \boldsymbol{F}_1(\boldsymbol{V}, \boldsymbol{\theta}, \boldsymbol{\psi_V}) \\ \dfrac{\mathrm{d}\boldsymbol{E_u}}{\mathrm{d}t} = \boldsymbol{F}_2(\boldsymbol{\omega_x}, \boldsymbol{\omega_y}, \boldsymbol{\omega_z}, \boldsymbol{\gamma}, \boldsymbol{\vartheta}) \\ \dfrac{\mathrm{d}m}{\mathrm{d}t} = -m_c \\ 0 = \boldsymbol{F}_3(\alpha, \beta, \gamma_V, \theta, \gamma, \varphi, \varphi_V, \vartheta) \\ 0 = \boldsymbol{F}_4(\delta_P, \delta_x, \delta_y, \delta_z) \end{cases} \tag{1}$$

where $\boldsymbol{V}$ denotes the vector of body velocity, $\boldsymbol{F}$ the external forces on body, $\boldsymbol{P}$ the propulsion force, $\boldsymbol{H}$ the moment of momentum, $\boldsymbol{M}$ the moment of force, $\boldsymbol{X_p}$ the position, $\boldsymbol{E_u}$ the Euler angles. $\boldsymbol{F}_1$, $\boldsymbol{F}_3$, $\boldsymbol{F}_3$, $\boldsymbol{F}_4$ denotes the functional relation of velocity, angular velocity, angular between four necessary coordinates and input. The parameters are sufficient to describe motion of a fixed-wing UAV. However, nonlinearity of the system is complicated and simplification under ideal condition is required.

The dynamics of a fixed-wing UAV can be simplified by letting $\omega_x = \omega_y = \omega_z = 0$, which means the ideal trajectory can be focused. Specifically, motion on horizontal plane can be modeled as follows by letting $y = 0$:

$$\begin{cases} m\dot{v} = P - X \\ mg = P\alpha_B + Y_B \\ -mV\dot{\psi_V} = -P\beta_B + Z_B \\ \dot{x} = V\cos\psi_V \\ \dot{z} = -V\sin\psi_V \\ \dot{m} = -m_c \\ \psi = \psi_V + \beta_B \\ \alpha_B = \vartheta \\ \varepsilon_2(\delta_x) = 0 \\ \varepsilon_4(\delta_P) = 0 \end{cases} \tag{2}$$

Let $x_i(t) = [x(t), z(t), v(t), \psi_V(t)]^T$, $u_i(t) = [P, \beta_B]^T$, obtaining a linearized system (3) under at operating points

(x_0, u_0) with the involvement of the Taylor series expansion as follows:

$$\dot{x}_i(t) = \begin{bmatrix} 0 & 0 & \cos\psi_V & -V\sin\psi_V \\ 0 & 0 & -\sin\psi_V & -V\cos\psi_V \\ 0 & 0 & 0 & 0 \\ 0 & 0 & \frac{-P\beta_B+Z_B}{mV^2} & 0 \end{bmatrix} x_i(t) + \begin{bmatrix} 0 & 0 \\ 0 & 0 \\ \frac{1}{m} & 0 \\ \frac{\beta_B}{mV} & \frac{P}{mV} \end{bmatrix} u_i(t) + \boldsymbol{F}(x_0, u_0) \tag{3}$$

where $\boldsymbol{F}(x_0, u_0)$ is the constant containing generally the aero-dynamics parameters estimation [41], representing general disturbance on a fixed-wing UAV without disturbance observer. For a tracking situation under trajectory $r_i(t)$, the complete system could be described as follows:

$$\begin{cases} \dot{x}_i(t) &= Ax_i(t) + Bu_i(t) + d_i(t) \\ e_i(t) &= Cx_i(t) + Du_i(t) - r_i(t) \end{cases} \tag{4}$$

where $d_i(t)$ is the equivalent disturbance of the whole system. To be specific, in this work leader-follower structure is adopted to form the formation, where $r_i(t)$ exists for the leader to trace and $r_i(t) = 0$ for the followers. $e_i(t) = [x_i(t), z_i(t)]^T$ denotes the output of a fixed-wing UAV, which is used for path tracking. Let $v_i(t) = col(r_i(t), d_i(t))$ to get a standard control system (A, B, C, D, E, F):

$$\begin{cases} \dot{x}_i(t) = Ax_i(t) + Bu_i(t) + Ev_i(t) \\ e_i(t) = Cx_i(t) + Du_i(t) + Fv_i(t) \end{cases} \tag{5}$$

where $x_i(t) \in \mathbb{R}^n, u_i(t) \in \mathbb{R}^m, e_i(t) \in \mathbb{R}^p, v_i(t) \in \mathbb{R}^q$. Subscript i represents fixed-wing UAV number in the formation. The compact form that transforms an individual system into formation form can be expressed as follows with Kronecker product:

$$\begin{cases} \dot{x}(t) = (I_N \otimes A)x(t) + (I_N \otimes B)u(t) + (I_N \otimes E)v(t) \\ e(t) = (I_N \otimes C)x(t) + (I_N \otimes D)u(t) + (I_N \otimes F)v(t) \end{cases} \tag{6}$$

where $x(t) = [x_1(t), x_2(t), \cdots, x_N(t)] \in \mathbb{R}^{Nn}$, $u(t) = [u_1(t), u_2(t), \cdots, u_N(t)] \in \mathbb{R}^{Nm}$, $e(t) = [e_1(t), e_2(t), \cdots, e_N(t)] \in \mathbb{R}^{Np}$, $v(t) = [v_1(t), v_2(t), \cdots, v_N(t)] \in \mathbb{R}^{Nq}$ denote the complete formation vector; "N" denotes the quantity of UAVs, "$\otimes$" denotes the Kronecker product, which combines formation states with individual UAV states. In addition, actuator multiplicative faults are mainly considered and could be modeled as follows:

$$u_i^f(t) = (I_m - \mu)u_i(t) \tag{7}$$

where μ denotes the actuator fault rate diagonal matrix with $0 \le \mu_{ii} \le 1$. Inspired by [42], the system with multiplicative actuator faults could be modeled in additive form as follows:

$$\dot{x}_i(t) = Ax_i(t) + Bu_i(t) + Ev_i(t) + f_{ai}(u)$$

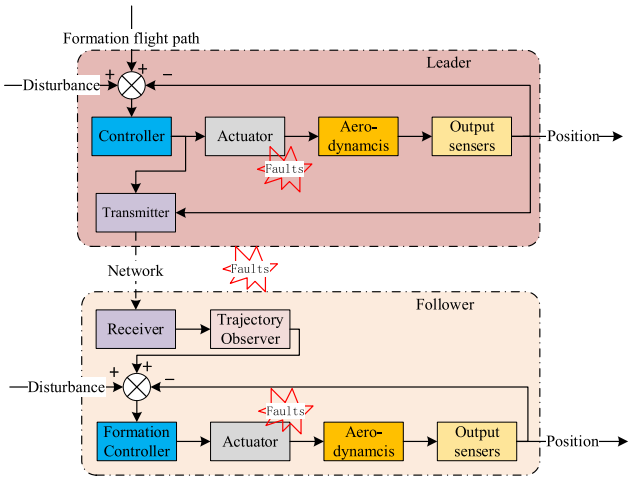

FIGURE 2. Block diagram of the formation between the leader and the followers.

where $f_{ai}(u) = -\mu Bu_i(t)$. Considering the saturation of actuator as redundant fault values, which is inspired by [29], let $D_a = diag(\overline{|u_i|}) \in \mathbb{R}^{m\times m}$, where $\overline{|u_i|}$ is the bound of the input. Then let $B_a = BD_a, \omega_{ai}(t) = -\mu D_{ai}^{-1}u_i(t)$, the compact formation form with fault model should be as follows:

$$\begin{cases} \dot{x}(t) &= (I_N \otimes A)x(t) + (I_N \otimes B)u(t) + (I_N \otimes E)v(t) \\ &\quad +(I_N \otimes B_a)\omega_a(t) \\ e(t) &= (I_N \otimes C)x(t) + (I_N \otimes D)u(t) + (I_N \otimes F)v(t) \end{cases} \tag{8}$$

where $\omega_a(t) = [\omega_{a1}(t), \omega_{a2}(t), \cdots, \omega_{aN}(t)]^T$ denotes the additive fault that derives from the transformation of actuator faults. In the system, $|\omega_{ai}(t)| = |-\mu D_{ai}^{-1}u_i(t)| < 1$ holds for general situation like faults. For saturation, the fault rate satisfies $\mu = I_m - \text{diag}(\overline{|u_i|}/u_i(t))$ and the modeled fault is $|\omega_{ai}(t)| = |(u_i(t)/\overline{|u_i|}) - 1_m|$.

Based on the model construction aforementioned, the following necessary assumption is required in this work.

Assumption 1: (A, B) is controllable and B is full column rank; (A, C) is detectable.

Remark 1: Based on the characteristics of Kronecker product, it is easily obtained that $(I_N \otimes A, I_N \otimes B)$ and $(I_N \otimes A, I_N \otimes C)$ are controllable and detectable if (A, B) and (A, C) are controllable and detectable.

The main formation structure is shown in Fig. 2, where relationships between the leader and the followers are depicted. To realize the formation control, some other important theories need to be briefly introduced, like output regulation theory and graph theory.

B. LINEAR OUTPUT REGULATION

Linear output regulation method proposed in [43] could be utilized to handle the disturbance whose form is as follows:

$$\dot{v}(t) = A_1 v(t) \tag{9}$$

The solution can be used to trace the trajectory like Dubins path and address the external disturbances, which depends on the form of A_1.

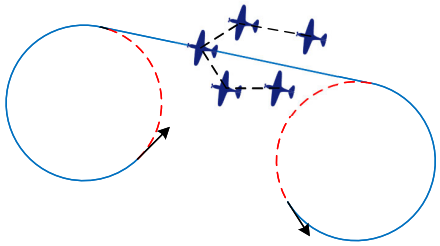

FIGURE 3. General Dubins path used in trajectory planning.

Remark 2: Generally speaking, as Fig. 3 shows, a Dubins path could be used for trajectory designing [44], where $A_1 = \begin{bmatrix} 0 & -\omega \\ \omega & 0 \end{bmatrix}$ *or* $A_1 = \frac{1}{t} I_{q\times q}$. *As for the constant disturbance like non-equilibrated operating points and constant part of aerodynamic resistance, it could be obtained that* $A_1 = 0_{q\times q}$.

Lemma 1: if

1) A_1 *has no eigenvalues with negative real parts,*

2) *the pair* (A, B) *is controllable*

then the output regulation equation (10) is solvable, which means the solution (X,U) exists.

$$\begin{cases} XA_1 &= AX + BU + E \\ 0 &= CX + DU + F \end{cases} \tag{10}$$

Let $\bar{x}_i(t) = x_i(t) - Xv_i(t), u_i(t) = K_x x_i(t) + K_v v_i(t)$, thorough (10) the closed-loop system with form (5) and internal model could be transformed:

$$\begin{cases} \dot{\bar{x}}_i(t) &= A_c \bar{x}_i(t) \\ e_i(t) &= C_c \bar{x}_i(t) + (C_c X + D_c) v_i(t) \end{cases} \tag{11}$$

where $A_c = A + BK_x, C_c = C + DK_x, D_c = F + DK_v$. The problem is therefore defined as follows:

Definition 1 (Linear Output Regulation Problem): Design a control law of state feedback or output feedback such that the closed-loop system (11) satisfies that A_c *is Hurwitz and* $\lim_{t\to\infty} e(t) = 0$.

By lemma 1 and analysis aforementioned, the algorithm could be concluded as follows.

Algorithm 1 Calculation of Output Regulation Method

Input: (A, B, C, D, E, F);
Output: K_v;
  for all $K_x \in \mathbb{R}^{m\times n}$ **do**
    compute $A_c = A + B * K_x$;
  end for
  A_c is Hurwitz;
  solve (10) to get solution (U, X);
  compute feedforward gain $K_v = U - XK_x$;
  return K_v.

Remark 3: A_c *under feedback gain* K_x *is Hurwitz, which is dependent from output regulation. The main function of output regulation equation is to make certain disturbance the internal model, which is derived from the control law* $u = K_x x + K_v v$. *The solution fits the trajectory-tracing problem. However, it requires the disturbance holds certain conditions in lemma 1. For those which do not match assumptions of lemma 1, for example, fault signal in this work, other method should be considered, constituting the main work of this paper.*

TABLE 1. Four fault types included to demonstrate the scenarios mentioned.

Fault type	Model
1. Fault	$\mu_{ii} \in (0, 1)$
2. Saturation	$\mu_{ii} = 1 - \frac{u_m}{u_i}, u_i \notin [u_{min}, u_{max}]$
3. Failure	$\mu_{ii} = 1$
4. Communication fault	$rank(L) < N$

Lemma 2: For a block symmetric matrix $S = \begin{bmatrix} S_{11} & S_{12}^T \\ S_{12} & S_{22} \end{bmatrix}$, *the following assertions are equivalent*:

1) $S < 0$
2) $S_{11} < 0, \quad S_{22} - S_{12} S_{11}^{-1} S_{12}^T < 0$
3) $S_{22} < 0, \quad S_{11} - S_{12}^T S_{22}^{-1} S_{12} < 0$

C. GRAPH THEORY

Fig. 4 shows the difference between actual communication network and the control relation network. The graph theory could help to transform the relationship between UAVs into the control relation network which could be further utilized in control systems for a leader-follower formation.

Let $G = \{V, E, W\}$ represents the network between different UAVs, where $V = \{v_1, v_2, \ldots, v_N\}$ is the vertex set which describes the nodes of network, $E \subseteq V \times V$ is the edge set which describes the connectivity of network and W is the weight set which describes the weight of each wedge. $A_G = [a_{ij}] \in \mathbb{R}^{N\times N}$ denotes the adjacency matrix in G where $a_{ij} > 0$ if $(v_i, v_j) \in E$ and $a_{ij} = 0$ if $(v_i, v_j) \notin E$. $D_G = \text{diag}\{N_i\}$ denotes the degree matrix of G where N_i denotes the neighbor number of each node. Let $L = [l_{ij}] = D_G - A_G$ denotes the Laplacian matrix and describes the control relation network [45]. $\sigma(t)$ denotes switching signal for network reconfiguration, which happens out of accident like communication faults.

For a leader-follower formation, if the leader is regarded as dependent one from others. Let $\Delta = diag\{a_{0i}\}$ denotes the adjacency between the leader and other followers. The Laplacian matrix with switching signal should be as follows:

$$H_{\sigma(t)} = L_{\sigma(t)} + \Delta_{\sigma(t)} \tag{12}$$

Then we have an assumption as follows:

Assumption 2: The graph G is connected and undirected.

Remark 4: By assumption 2, considering the transceiver in each UAV, the graph G could be undirected, ensuring the symmetry of $H_{\sigma(t)}$. *Another way defining the Laplacian matrix could be* $L_{\sigma(t)} = \begin{bmatrix} 0 & 0 \\ L_{0\sigma(t)} & L_{\sigma(t)} \end{bmatrix}$ *where the leader and the follower are all regarded as one group. However, the symmetry of control connections would be missing,*

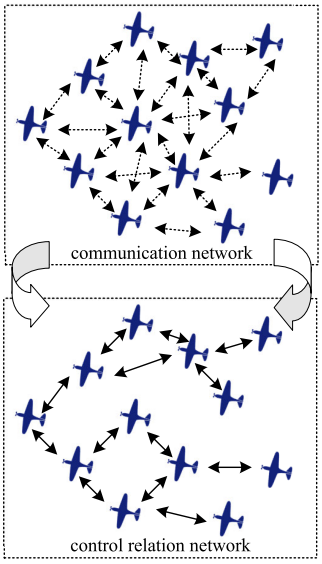

FIGURE 4. Using graph theory to transform communication network into control relation network.

contributing inconvenience to solutions, while the difficulty would be avoided by (12).

Above all the fault models that need to discuss in this paper can be summarized in Table. 1, including fault, saturation, failure and communication faults. u_m denotes the boundary of the inputs, when $u_i < u_{min}, u_m = u_{min}$ and when $u_i > u_{max}, u_m = u_{min}$. $rank(L) < N$ implies that the Laplacian matrix of the formation is not full rank, representing the communication faults.

III. MAIN RESULTS

Generally the state of the leader UAV is difficult to get access, an observer is used to estimate the states. The system of follower i in the formation should be as follows:

$$\begin{cases} \dot{x}_i(t) = Ax_i(t) + Bu_i(t) + d_i(t) \\ e_i(t) = Cx_i(t) + Du_i(t) \\ \dot{\hat{x}}_i(t) = A\hat{x}_i(t) + Bu_i(t) + d_i(t) - L(\hat{e}_i(t) - e_i(t)) \\ \hat{e}_i(t) = C\hat{x}_i(t) + Du_i(t) \end{cases} \tag{13}$$

where $\hat{x}_i$ and $\hat{e}_i$ denote the observer vectors for follower i to trace the trajectory of the leader. Define $\delta_i(t) = \hat{x}_i(t) - x_i(t)$ as error vector for a Luenberger Observer to estimate the state of UAV. The dynamics of error vector should be:

$$\dot{\delta}_i(t) = (A - LC)\delta_i(t) \tag{14}$$

Since (A, C) is detectable, gain matrix L exists to make $\delta_i(t)$ asymptotic stable.

In addition, formation vector $h_i(t) = [\Delta_{xi}, \Delta_{zi}, \Delta_{vi}, \Delta_{\psi Vi}]^T$ is required to make formation possible. Then the trace vector of formation tracking is defined, and the formation control problem should be described as follows:

Definition 2: $x_0(t)$ is the trajectory of leader, $x_i(t)$ is the trajectory of i-th follower, $h_i(t)$ is the formation vector of i-th follower. Call formation control problem is solved, if $\forall i \in N$, equation below holds:

$$\lim_{t\to\infty}(x_i(t) - x_0(t) - h_i(t)) = 0 \tag{15}$$

Define a trace vector by observer vectors $\Phi_i(t) = \hat{x}_i(t) - \hat{x}_0 - h_i(t)$, if $\lim_{t\to\infty} \Phi_i(t) = 0, \forall i \in N$. If $\lim_{t\to\infty} \delta_i(t) = 0$ under gain matrix L, it is also feasible to call the formation control problem is solved.

The consensus control method in the leader-follower formation is as follows:

$$u_i(t) = K[\sum_{j\in N} a_{ij}(\hat{x}_i(t) - \hat{x}_j(t)) + a_{i0}(\hat{x}_i - \hat{x}_0 - h_i(t))] + q_i(t) \tag{16}$$

The compact form should be:

$$u(t) = (H \otimes K)\Phi(t) + q(t) \tag{17}$$

It consists of two parts. The first is consistency part, which could be directly used in state feedback control and makes consensus control possible. The second is compensation part, which compensates certain known additional input like tracking vector and formation vector. It is necessary to state formation feasibility in advance.

Formation feasibility condition: Let $B' = [\hat{B}^T, \bar{B}^T]^T$ as a non-singular matrix which satisfies $\hat{B}B = I_{m\times m}$ and $\bar{B}B = 0_{(n-m)\times m}$. To directly compensate the formation factor $h_i(t)$, the compensation should satisfy $Bq_{1i}(t) + Ah_i(t) - \dot{h}_i(t) = 0$. Let $q_{1i} = -\hat{B}(Ah_i(t) - \dot{h}_i(t))$, and the formation feasibility condition should be as follows:

$$\bar{B}(Ah_i(t) - \dot{h}_i(t)) = 0 \tag{18}$$

which means $B'[Bq_{1i}(t) + Ah_i(t) - \dot{h}_i(t)] = 0$ holds for B' as a non-singular matrix, completing the compensation. It shows that direct compensation is limited. If the formation vector is fixed like those in classic scenarios, regulation equation can also be taken into consideration.

Definition 3 (Formation Consistency Problem): Design a control law of the form (17) in system (6) such that form (15) holds.

Theorem 1: Under the Graph of $H_{\sigma(t)}$, $\forall \lambda_{i\sigma(t)} \in \sigma(H_{\sigma(t)}), i = 1, \cdots, n$, if $(A, \lambda_{i\sigma(t)}B)$ is stabilized under control method (17), then it can be said that formation control problem is solved

Proof: The dynamics of trace vector $\Phi_i(t)$ is

$$\begin{aligned} \dot{\Phi}_i(t) &= \dot{\hat{x}}_i(t) - \dot{\hat{x}}_0(t) - \dot{h}_i(t) \\ &= A\hat{x}_i(t) + Bu_i(t) + d_i(t) - LC\delta_i(t) - (A\hat{x}_0(t) + Bu_0(t) \\ &\quad + E_0v_0(t) - LC\delta_0(t)) - \dot{h}_i(t) \\ &= A\Phi_i(t) + B\tilde{u}_i(t) + Ah_i(t) - \dot{h}_i(t) + d_i(t) \\ &\quad - E_0v_0(t) - LC\tilde{\delta}_i(t) \end{aligned}$$

where $\tilde{u}(t) = u_i(t) - u_0(t)$, $\tilde{\delta}_i(t) = \delta_i(t) - \delta_0(t)$, meaning the error of input vector and observer vector. The compact form is as follows:

$$\begin{aligned} \dot{\Phi}(t) &= (I_N \otimes A)\Phi(t) + (I_N \otimes B)\tilde{u}(t) + (I_N \otimes A)h(t) - \dot{h}(t) \\ &\quad + (I_N \otimes E)v(t) - (I_N \otimes LC)\tilde{\delta}(t) \end{aligned} \tag{19}$$

where $E = [E_0, I_q]$,$v(t) = \left\{[v_0(t), d_i(t)]^T\right\} (1 \le i \le N)$.And $v(t)$ submits $\dot{v}(t) = (I_N \otimes \bar{A}_1)v(t)$, where $\bar{A}_1 = \begin{bmatrix} A_{10} & \\ & 0 \end{bmatrix}$,in which A_{10} is the system matrix of $v_0(t)$

The control method (17) could be rewritten as follows in such a situation:

$$\tilde{u}(t) = (H_{\sigma(t)} \otimes K)\Phi(t) + q_1(t) + q_2(t) \tag{20}$$

where $q_1(t) = -\bar{B}(Ah(t) - \dot{h}(t))$ which is the compensation of formation according to formation feasibility condition, $q_2(t)$ is the feedforward compensation of $v(t)$.

Knowing that $H_{\sigma(t)}$ is symmetric positive matrix. $\exists M_{\sigma(t)} \in \mathbb{R}^{N\times N}, s.t. H_{\sigma(t)} = M^T_{\sigma(t)} \wedge_{\sigma(t)} M_{\sigma(t)}$,where $M_{\sigma(t)}$is orthogonal matrix and $\wedge_{\sigma(t)} = diag([\lambda_{1\sigma(t)}, \lambda_{2\sigma(t)}, \cdots, \lambda_{N\sigma(t)}])$ for $\lambda_{i\sigma(t)} \in \sigma(H_\sigma(t))$. Let $\eta(t) = (M^T_{\sigma(t)} \otimes I_n)\Phi(t)$. Then dynamics (19) with control method (20) transforms into:

$$\begin{aligned}\dot{\eta}(t) = (I_N \otimes A + \wedge_{\sigma(t)} \otimes BK)\eta(t) - (M^T_{\sigma(t)} \otimes LC)\tilde{\delta}(t)\\ + (M^T_{\sigma(t)} \otimes E)v(t) + (M^T_{\sigma(t)} \otimes B)q_2(t)\end{aligned} \tag{21}$$

For $M^T_{\sigma(t)} = \left\{m_{ij\sigma(t)}\right\}$, we have $\sum_{j=1}^N m_{ij\sigma(t)} = 1$. Let $\tilde{\delta}^M_{i\sigma(t)}(t) = \sum_{j=1}^N m_{ij\sigma(t)}\tilde{\delta}_i(t)$,$v^M_{i\sigma(t)}(t) = \sum_{j=1}^N m_{ij\sigma(t)}v_i(t)$, $q^M_{2i\sigma(t)}(t) = \sum_{j=1}^N m_{ij\sigma(t)}q_{2i}(t)$, $e^M_{i\sigma(t)}(t) = \sum_{j=1}^N m_{ij\sigma(t)}e_i(t)$. The compact form of the whole system should be as follows:

$$\begin{cases}\dot{\eta}(t) = (I_N \otimes A + \wedge_{\sigma(t)} \otimes BK)\eta(t) - (I_N \otimes LC)\tilde{\delta}^M_{\sigma(t)}(t)\\ \quad +(I_N \otimes E)v^M_{\sigma(t)}(t) + (I_N \otimes B)q^M_{2\sigma(t)}(t)\\ \dot{v}^M_{\sigma(t)}(t) = (I_N \otimes \bar{A}_1)v^M_{\sigma(t)}(t)\\ \tilde{\delta}^M_{\sigma(t)}(t) = (I_N \otimes (A - LC))\tilde{\delta}^M_{\sigma(t)}(t)\\ e^M_{\sigma(t)}(t) = (I_N \otimes C)\eta(t)\end{cases} \tag{22}$$

Equation (22) then could return to separated form as follows:

$$\begin{cases}\dot{\eta}_i(t) = (A + \lambda_{i\sigma(t)}BK)\eta_i(t) - LC\tilde{\delta}^M_{i\sigma(t)}(t)\\ \quad +Ev^M_{i\sigma(t)}(t) + Bq^M_{2i\sigma(t)}(t)\\ \dot{v}^M_{i\sigma(t)}(t) = \bar{A}_1 v^M_{i\sigma(t)}(t)\\ \tilde{\delta}^M_{i\sigma(t)}(t) = (A - LC)\tilde{\delta}^M_{i\sigma(t)}(t)\\ e^M_{i\sigma(t)}(t) = C\eta_i(t)\end{cases} \tag{23}$$

Equation (23) under consensus control method (20) is equivalent to a new switching system $(A, \lambda_{i\sigma(t)}B)$ by general state feedback control. If $\lim_{t\to\infty} \eta_i(t) = 0, \forall i \in N$,according to $\eta(t) = (M^T_{\sigma(t)} \otimes I_n)\Phi(t)$, then $\lim_{t\to\infty} \Phi(t) = 0$, Theorem 1 holds by definition 2. □

Remark 5: The most important role in consensus method is the consensus part $(H_{\sigma(t)} \otimes K)\Phi(t)$, which makes the consensus control possible as if output error in Luenberger Observer. $(M^T_{\sigma(t)} \otimes I_n)$ in other part of dynamics of $\Phi(t)$ is utilized for equalization or reconfiguration of other signals and has few effects on stability of the system. By disassembling the consensus problem as separated one, the eigenvalues $\lambda_{i\sigma(t)}$ of $H_{\sigma(t)}$ are essential factors to construct an equivalent amplification system compared to original one, which means switching topologies have similar effect on a system like actuator faults, instead of switching system proposed in [36].

Definition 4 (Formation Consensus Fault-Tolerant Control Problem): Design a control law of the form (17) in system (8) such that form (15) holds.

Then we get the system as follows:

$$\begin{cases}\dot{\Phi}(t) &= (I_N \otimes A)\Phi(t) + (I_N \otimes B)\tilde{u}(t) - (I_N \otimes LC))\tilde{\delta}(t)\\ &\quad +(I_N \otimes E)v(t) + (I_N \otimes B_a)\omega_a(t)\\ \dot{v}(t) &= (I_N \otimes \bar{A}_1)v(t)\\ \tilde{\delta}(t) &= (I_N \otimes (A - LC))\tilde{\delta}(t)\\ e(t) &= (I_N \otimes C)\Phi(t)\end{cases} \tag{24}$$

Theorem 2: Formation system (24) has a fault-tolerant control gain K, if and only if LMI (25) has solution $(Y^*, W^*), \forall\lambda_{i\sigma(t)} \in \sigma(H_{\sigma(t)})$, where the state feedback gain $K = W^*(Y^*)^{-1}$.

$$\begin{bmatrix}\Xi_1(\lambda) & -LC & B_a & (CY)^T\\ * & \Xi_2 & 0 & 0\\ * & * & -I & 0\\ * & * & * & -\gamma^2 I\end{bmatrix} < 0 \tag{25}$$

where $\Xi_1(\lambda) = AY + \lambda_{i\sigma(t)}BW + (AY + \lambda_{i\sigma(t)}BW)^T$ and $\Xi_2 = (A - LC) + (A - LC)^T$.

Proof: By Theorem 1, system (24) could be reform to an equivalent one as follows:

$$\begin{cases}\dot{\eta}_i(t) = (A + \lambda_{i\sigma(t)}BK)\eta_i(t) - LC\tilde{\delta}^M_{i\sigma(t)}(t) + Ev^M_{i\sigma(t)}(t)\\ \quad +Bq^M_{2i\sigma(t)}(t) + B_a\omega^M_{ai\sigma(t)}(t)\\ \dot{v}^M_{i\sigma(t)}(t) = \bar{A}_1 v^M_{i\sigma(t)}(t)\\ \tilde{\delta}^M_{i\sigma(t)}(t) = (A - LC)\tilde{\delta}^M_{i\sigma(t)}(t)\\ e^M_{i\sigma(t)}(t) = C\eta_i(t)\end{cases} \tag{26}$$

where i denotes the $i - th$ UAV. By algorithm 1, robust regulation equation of system (26) should be as follows:

$$\begin{cases}X_i\bar{A}_1 = AX_i + \lambda_{i\sigma(t)}BU_i + E\\ 0 = CX_i\end{cases} \tag{27}$$

where the solution is $(U_{i\sigma(t)}, X_{i\sigma(t)})$. Then distributed feedforwad gain $K^M_{vi\sigma(t)} = U_{i\sigma(t)} - X_{i\sigma(t)}K$. Let $\bar{\eta}_i(t) = \eta_i(t) - X_{i\sigma(t)}v^M_{i\sigma(t)}(t)$. The whole system should be rewritten as follows:

$$\begin{cases}\dot{\bar{\eta}}_i(t) = (A + \lambda_{i\sigma(t)}BK)\bar{\eta}_i(t) - LC\tilde{\delta}^M_{i\sigma(t)}(t) + B_a\omega^M_{ai\sigma(t)}(t)\\ \tilde{\delta}^M_{i\sigma(t)}(t) = (A - LC)\tilde{\delta}^M_{i\sigma(t)}(t)\\ e^M_{i\sigma(t)}(t) = C\eta_i(t)\end{cases} \tag{28}$$

Let $z_{i\sigma(t)}(t) = col(\bar{\eta}_i(t), \tilde{\delta}^M_{i\sigma(t)}(t))$. The composite system will be as follows:

$$\begin{cases}\dot{z}_{i\sigma}(t) = (\bar{A} + \lambda_{i\sigma(t)}\bar{B}K)z_{i\sigma(t)}(t) + \bar{B}_a\omega^M_{ai\sigma(t)}(t)\\ e^M_{i\sigma(t)}(t) = \bar{C}\eta_i(t)\end{cases} \tag{29}$$

where $\bar{A} = \begin{bmatrix} A & -LC \\ 0 & A-LC \end{bmatrix}$, $\bar{B} = \begin{bmatrix} B \\ 0 \end{bmatrix}$, $\bar{B}_a = \begin{bmatrix} B_a \\ 0 \end{bmatrix}$, $\bar{C} = [C, 0]$, which consists of a new system $(\bar{A}, \bar{B}, \bar{C}, 0, \bar{B}_a, 0)$. The bounded fault vector $\omega^M_{ai\sigma(t)}(t)$ has no specific dynamics equation. H_∞ control method should be taken into consideration to realize the robustness of control system.

Let $\bar{P} = \begin{bmatrix} P & \\ & I \end{bmatrix}$ and define a Lyapunov function as follows:

$$V(t) = z^T_{i\sigma(t)}(t)\bar{P}z_{i\sigma(t)}(t) \tag{30}$$

Then the time derivative of (30) could be calculated as follows:

$$\begin{aligned}\dot{V}(t) = {} & z^T_{i\sigma(t)}[(\bar{A} + \lambda_{i\sigma(t)}\bar{B}\bar{K})^T\bar{P} + \bar{P}(\bar{A} + \lambda_{i\sigma(t)}\bar{B}\bar{K})]z_{i\sigma(t)} \\ & + z^T_{i\sigma(t)}\bar{P}\bar{B}_a\omega_{ai\sigma(t)} + \omega^T_{ai\sigma(t)}\bar{B}^T_a\bar{P}z_{i\sigma(t)}\end{aligned} \tag{31}$$

To realize $\dot{V}(t) < 0$, the inequation as follows should hold:

$$\begin{bmatrix} (\bar{A} + \lambda_{i\sigma(t)}\bar{B}\bar{K})^T\bar{P} + \bar{P}(\bar{A} + \lambda_{i\sigma(t)}\bar{B}\bar{K}) & \bar{P}\bar{B}_a & (\bar{C})^T \\ * & -I & 0 \\ * & * & -\gamma^2 I \end{bmatrix} < 0 \tag{32}$$

Let $\bar{Y} = \bar{P}^{-1} = \begin{bmatrix} Y & \\ & I \end{bmatrix}$ and $\bar{W} = [W, 0]$, then multiply a matrix $diag\{\bar{P}^{-1}, I, I\}$ from both sides, transforming (32) into the one as follows:

$$\begin{bmatrix} \Xi_1(\lambda) & -LC & B_a & (CY)^T \\ * & \Xi_2 & 0 & 0 \\ * & * & -I & 0 \\ * & * & * & -\gamma^2 I \end{bmatrix} < 0 \tag{33}$$

where $\Xi_1(\lambda) = AY + \lambda_{i\sigma(t)}BW + (AY + \lambda_{i\sigma(t)}BW)^T$ and $\Xi_2 = (A - LC) + (A - LC)^T$.

Based on Lemma 2, if LMI (33) holds, then next LMI also holds:

$$AY + \lambda_{i\sigma(t)}BW + (AY + \lambda_{i\sigma(t)}BW)^T < 0 \tag{34}$$

Then the derivative of Lyapunov function would be $\dot{V}(t) < 0$ where $K = WY^{-1}$ if letting $\omega_{ai\sigma(t)} = 0$, which means the states of the system is asymptotically stable. Based on definition 2, formation control problem is guaranteed. If $\omega_{ai\sigma(t)} \neq 0$, meaning actuator faults happen, H_∞ performance should be described as follows:

$$\Gamma_{i\infty}(T) = \frac{\int_T z^T_{i\sigma(t)}(t)z_{i\sigma(t)}(t)\mathrm{d}t - z^T_{i\sigma(t)}(0)\bar{P}z_{i\sigma(t)}(0)}{\int_T \omega^T_{ai\sigma(t)}(t)\omega_{ai\sigma(t)}(t)\mathrm{d}t} \tag{35}$$

Let $J_i(T) = \int_T (z^T_{i\sigma(t)}(t)z_{i\sigma(t)}(t) - \gamma^2\omega^T_{ai\sigma(t)}(t)\omega_{ai\sigma(t)}(t))\mathrm{d}t$, then we have:

$$\begin{aligned} J_i(T) = {} & \int_T (z^T_{i\sigma(t)}(t)z_{i\sigma(t)}(t) - \gamma^2\omega^T_{ai\sigma(t)}(t)\omega_{ai\sigma(t)}(t) \\ & + \dot{V}(t))\mathrm{d}t - V(T) + V(0) \\ = {} & \int_T (\begin{bmatrix} z_{i\sigma(t)}(t) \\ \omega^T_{ai\sigma(t)}(t) \end{bmatrix}^T (\begin{bmatrix} \bar{A}^T\bar{P} + \bar{P}\bar{A} & \bar{P}\bar{B}_a \\ * & -\gamma^2 I \end{bmatrix} \\ & + \begin{bmatrix} \bar{C}^T \\ 0 \end{bmatrix}[\bar{C} \quad 0]) \begin{bmatrix} z_{i\sigma(t)}(t) \\ \omega^T_{ai\sigma(t)}(t) \end{bmatrix})\mathrm{d}t - V(T) \end{aligned} \tag{36}$$

Let $T \to \infty$, according to LMI (32) we have:

$$\begin{aligned} J_i(\infty) = {} & \int_\infty z^T_{i\sigma(t)}(t)z_{i\sigma(t)}(t) - \gamma^2\omega^T_{ai\sigma(t)}(t)\omega_{ai\sigma(t)}(t)\mathrm{d}t \\ & - V(0) < 0 \end{aligned} \tag{37}$$

which means $\Gamma_{i\infty}(\infty) < \gamma^2$ and robustness of the system is guaranteed, finishing the proof. □

In conclusion, an algorithm to calculate the control law is presented below:

Algorithm 2 Calculation of Formation Robust Fault-Tolerant Control (FRFTC)

Input: (A, B, C, D, E, F) and $H_{\sigma(t)}$;
Output: K_v and $q_2(t)$;
compute $H_{\sigma(t)} = M^T_{\sigma(t)} \wedge_{\sigma(t)} M_{\sigma(t)}$;
solve equation (33), $\forall\lambda_{i\sigma(t)} \in \rho(H_{\sigma(t)})$;
solve inequality (25) to get the formation fault-tolerant control gain K;
solve equation (27), $\forall\lambda_{i\sigma(t)} \in \rho(H_{\sigma(t)})$;
get distributed solution $(U_{i\sigma(t)}, X_{i\sigma(t)})$;
get feedforward gain $K^M_{vi\sigma(t)} = U_{i\sigma(t)} - X_{i\sigma(t)}K$;
get feedforwatd compensation $q_2(t) = (M_{\sigma(t)} \otimes I_n)(K_{v\sigma(t)}v^M_{\sigma(t)}(t))$;
return K_v and $q_2(t)$.

Remark 6: The switching topologies play the role of switching input gain while the actuator faults the role of disturbances. The method focuses on passive fault-tolerant control by making actuator faults under saturation equivalent to bounded disturbance to fulfill the cooperative performance needed, which means a trade-off between performance and robustness has to be made. Besides, LMI (25) in theorem 2 provides a sufficient solution and the scalar γ can be adjusted to enlarge the feasible region to get access to formation feedforward gain K. The solvability depends on the structure of the formation system.

IV. SIMULATION

In Simulation, the proposed FRFTC method is demonstrated on a group of four followers and one leader. To verge on the actual scenario, $x_0(t) = [0, 0, 10\pi, 0]^T$ and $u_0(t) = [10, 0]^T$, which means the initial velocity of around 30 m/s and the initial propulsion of 10 N, are set to be the operating points, obtaining a controllable and detectable system as follows. As for the communication network, the chosen switching graphs G with one leader and four followers are full-connected and line-connected ones as Fig. 5 and Fig. 6 show.

$$\begin{aligned} A = {} & \begin{bmatrix} 0 & 0 & 1 & 0 \\ 0 & 0 & 0 & 3.1416 \\ 0 & 0 & 0 & 0 \\ 0 & 0 & 0.0101 & 0 \end{bmatrix}, \quad B = \begin{bmatrix} 0 & 0 \\ 0 & 0 \\ 0.1 & 0 \\ 0 & 1 \end{bmatrix} \\ C = {} & \begin{bmatrix} 1 & 0 & 0 \\ 0 & 1 & 0 & 0 \end{bmatrix}, \quad D = \mathbf{0}_{p\times m} \end{aligned} \tag{38}$$

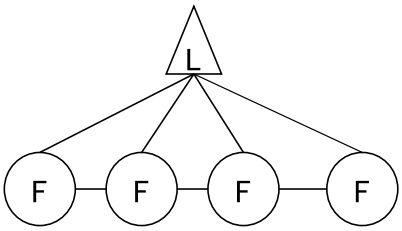

FIGURE 5. Full-connected network communication topology.

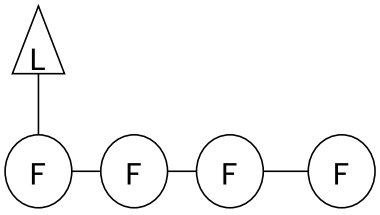

FIGURE 6. Line-connected network communication topology.

TABLE 2. Scenarios with different faults.

Scenario number	Condition
1. Fault 1	$\mu_P = 0.1, \mu_{\beta_B} = 0.1$
2. Fault 2	$\mu_P(t) = 0.9\sin^2(\frac{\pi}{20}t), \mu_{\beta_B}(t) = 0.9\cos^2(\frac{\pi}{20}t)$
3. Saturation	$u_{P,min} = -45, u_{P,max} = 45; u_{\beta_B,min} = -1, u_{\beta_B,max} = 1$
4. Failure	$\mu_P = 1, \mu_{\beta_B} = 1$
5. Communication switch 1	From full-connected network to line-connected network
6. Communication switch 2	From line-connected network to full-connected network
7. Communication fault	Loss of Network of UAV 4

As shown in Table. 2, a total of seven fault scenarios are designed by synthesizing the different fault types discussed. Scenarios 1 and 2 represent general efficiency failure scenarios, respectively, distinguishing between fixed and time-varying failures; Scenario 3 represents actuator saturation failures; Scenario 4 represents failures at a failure rate of 1, where the form of the failure rises to the formation system, and thus correlates with the communication state of the whole system, on top of which we consider topology changes. Scenarios 5 and 6 represent different topology switches, alternating between full connectivity to line connectivity, respectively. Scenario 7, on the other hand, considers UAV communication breaks. UAV failures will be injected into the system at $t = 20$ s in all simulations and communication failures will be injected into the system at $t = 10$ s in different hybrid scenarios to validate the effectiveness of the algorithm.

Fig. 7 shows the trajectory as a circle dubins path which the leader follows, where $A_1 = \begin{bmatrix} 0 & -\pi/10 \\ \pi/10 & 0 \end{bmatrix}$ and radius is 200 m, which is the general scale of fixed-wing UAV flight compared to 1∼2 m of fixed-wing UAV itself. The time-invariant formation vector for each UAV is $h_1 = [10, 10, 0, 0]^T$, $h_2 = [20, 20, 0, 0]^T$, $h_3 = [30, 30, 0, 0]^T$,$h_4 = [40, 40, 0, 0]^T$, which is the line-like formation and satisfies the formation feasibility condition (18), where $Ah_i(t) - \dot{h}_i(t) \in \ker(\bar{B})$.

The simulation results are divided into four parts according to 4 main Scenarios selected from Table. 2 by tracking the ideal formation, including faults, saturation and the mixed

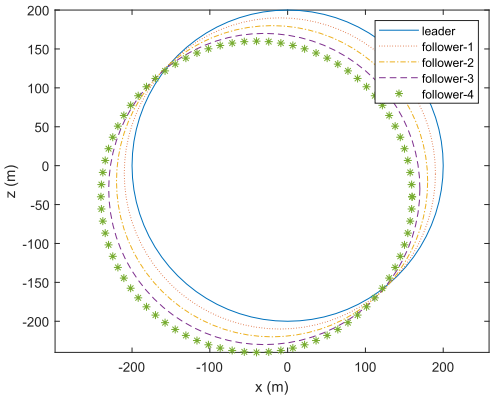

FIGURE 7. The ideal trajectory of the formation.

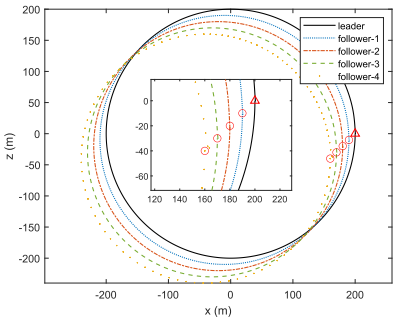

(a) The trajectory of the formation in scenario 2 and 5.

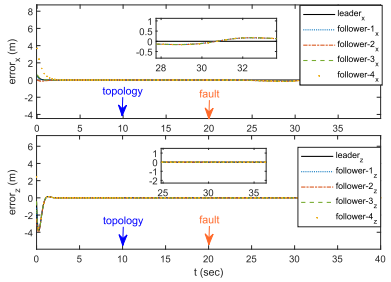

(b) The errors of the formation in scenario 2 and 5.

FIGURE 8. Tracking results of the formation in scenario 2 and 5.

scenarios with switching topologies. Fig. 8 - Fig. 11 show the actual trajectory of formation and the errors in x and z directions respectively with the proposed FRFTC method. It can be seen that topology faults are equivalent to a change in the control gain and do not affect the stability of the formation since it is addressed by the FRFTC method. For faults, the change in error is faint when the faults are in the form of general multiplicative faults. However, when the system is considered saturation, the errors of the flight will be stretched out and large deviations from the UAV scale will occur. When saturation with fault 1 happens, the formation remains stable to some extent, but when saturation with fault 2 happens, the formation is affected not only by the deviation from the scale of the UAV itself but also by the whole trajectory of the formation. Therefore, the proposed algorithm can cope with the proposed faults separately, but when multiple faults are combined, the stability of the system will be greatly

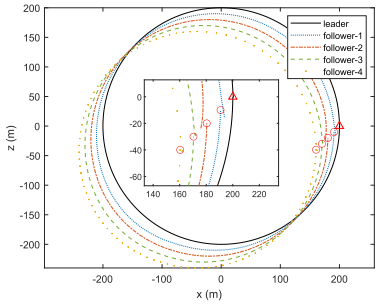

(a) The trajectory of the formation in scenario 3 and 6.

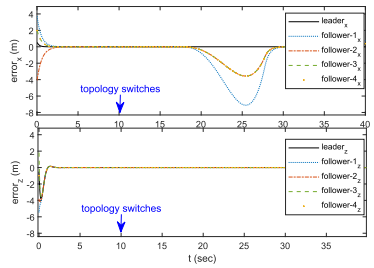

(b) The errors of the formation in scenario 3 and 6.

FIGURE 9. Tracking results of the formation in scenario 3 and 6.

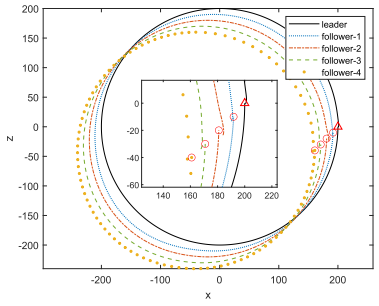

(a) The trajectory of the formation in scenario 1, 3 and 6.

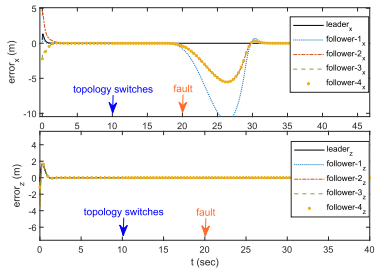

(b) The errors of the formation in scenario 1, 3 and 6.

FIGURE 10. Tracking results of the formation in scenario 1, 3 and 6.

challenged since the saturation is nonlinear fault and would adversely affect the system. Fig. 12 shows the impact of saturation without faults on Follower 1, where the inputs reach the boundaries and result in tracking errors like faults in Fig. 9.

To better characterize the performance deviations of the UAV formation not only in terms of the stability of the

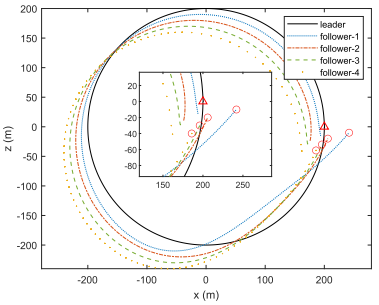

(a) The trajectory of the formation in scenario 2, 3 and 6.

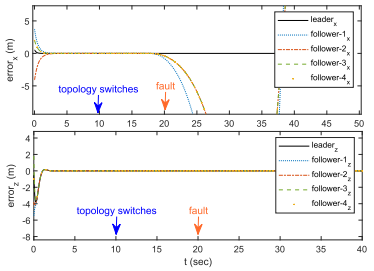

(b) The errors of the formation in scenario 2, 3 and 6.

FIGURE 11. Tracking results of the formation in scenario 2, 3 and 6.

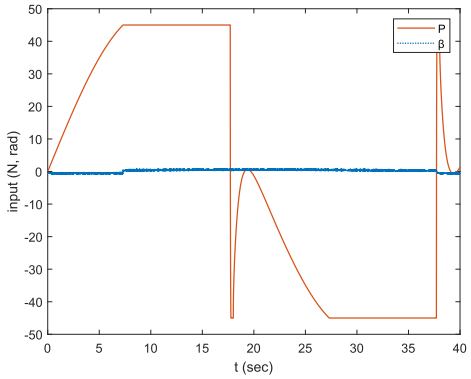

FIGURE 12. Input of follower 1 in the formation with saturation.

individual UAV but also in terms of the stability of the system, inspired by failure thresholds proposed in [42] and practical work, an optimal evaluation of the failure state is obtained by using a calculation of the L2 norm of each trajectory error in the period of 20 s-40 s. In (39), accumulated cooperative error (ACE) as the average of L2 norm of the followers' errors is proposed to represent system performance. At the same time, comparison is made with a general formation LQR (FLQR) algorithm proposed in [24] and [30]. The algorithm is often used as basis for formation flying under different assumptions by Riccati inequalities $A^TQ+QA-2\epsilon_{min}QBB^TQ+\epsilon_{min}I < 0$, where ϵ_{min} denotes the minimum eigenvalue of $H_{\sigma(t)}$ in (12) and the feedback gain satisfies $K = B^TQ$.

$$J_{ACE} = \frac{1}{N}\sum_{i=1}^{N} \| e_i(k) \|_2^2 = \frac{1}{N}\sum_{i=1}^{N}\sum_{j=1}^{M} \| e_i(k+j) \|_2^2 \quad (39)$$

TABLE 3. Comparison of errors and accumulated cooperative error in $T \in [20s, 40s]$ between FLQR and FRFTC in different scenarios.

Method	Scenario	$\|\| L_x \|\|_2^2$	$\|\| L_z \|\|_2^2$	$\|\| F1_x \|\|_2^2$	$\|\| F1_z \|\|_2^2$	$\|\| F2_x \|\|_2^2$	$\|\| F2_z \|\|_2^2$	$\|\| F3_x \|\|_2^2$	$\|\| F3_z \|\|_2^2$	$\|\| F4_x \|\|_2^2$	$\|\| F4_z \|\|_2^2$	$\|\| \cdot \|\|_2^2$
FLQR	2&5	0.00	0.00	1.16	6.30	1.17	6.40	1.18	6.47	1.18	6.51	3.04
	1&6	0.00	0.00	0.06	0.34	0.03	0.17	0.03	0.17	0.03	0.17	0.10
	2&6	0.00	0.00	0.56	2.97	0.28	1.49	0.28	1.49	0.28	1.49	0.88
	3&6	0.00	0.00	238.70	0.00	119.41	0.00	119.41	0.00	119.41	0.00	59.69
	1&3&6	0.00	0.00	394.56	0.01	197.52	0.01	197.52	0.01	197.52	0.01	98.71
	2&3&6	0.00	0.00	2737.8	0.00	1369.2	0.00	1369.2	0.00	1369.2	0.00	684.55
FRFTC	2&5	0.00	0.00	4.49	0.14	4.57	0.14	4.63	0.14	4.66	0.14	1.89
	1&6	0.00	0.00	0.21	0.01	0.10	0.00	0.10	0.00	0.10	0.00	0.05
	2&6	0.00	0.00	2.09	0.07	1.05	0.03	1.05	0.03	1.05	0.03	0.54
	3&6	0.00	0.00	192.97	0.01	96.63	0.01	96.63	0.01	96.63	0.01	48.29
	1&3&6	0.00	0.00	316.07	0.01	158.25	0.01	158.25	0.01	158.25	0.01	79.08
	2&3&6	0.00	0.00	2202.4	0.00	1.102	0.00	1101.8	0.00	1101.8	0.00	550.80

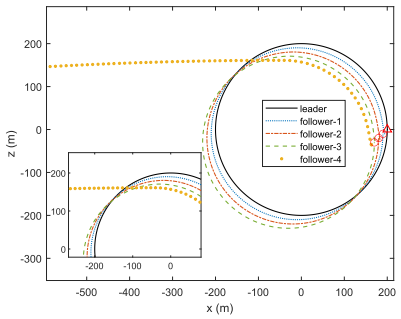

(a) The trajectory of the formation in scenario 7.

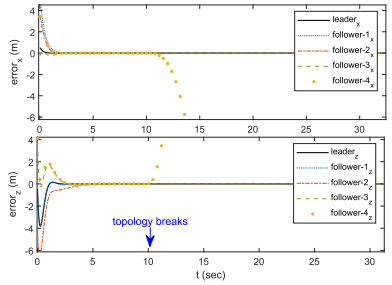

(b) The errors of the formation in scenario 7.

FIGURE 13. The topology follower 4 breaks in scenario 7.

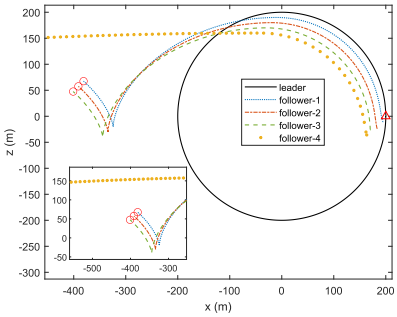

(a) The failure with $\mu = 1$ is injected into the UAV 4 as scenario 4.

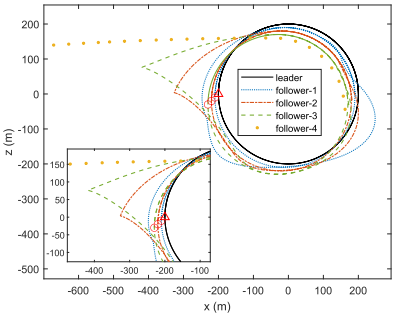

(b) The topology of UAV 4 breaks 5s after the failure is injected.

FIGURE 14. Failure with topology break in scenario 4 and 7.

Simulation statistics in scenarios from Table. 2 are shown in Table. 3, where the unit of the data is m^2 as practical situations. For the FRFTC method, by comparing fault 2 with different topology types (2&5 vs. 2&6), it can be found that the communication of the formation itself provides robustness to the system, where the ACEs are 1.89 m^2 in line-connected topology and 0.05 m^2 in full-connected topology respectively. In the same topology switching form, as the severity of faults deepens, the system becomes more unstable and oscillatory. In particular, it is important to note that the errors of the followers and the ACE of the whole system violently increase from 48.29 m^2 to 79.08 m^2 when saturation meets fault 1, which shows the conservatism of the proposed method. Nevertheless, according to the data comparison, FRFTC has a significant suppression effect compared with FLQR, which verifies the effectiveness of the proposed formation performance.

However, there are more application scenarios for the present algorithm to address the problem when the attention rises to the formation level. Fig. 13 represents a complete UAV communication break, which is equivalent to a complete loss of a UAV, and it can be noticed from Fig. 13(a) that when UAV 4 is injected with a communication break at $t = 10$ s, the UAV goes out of control due to the unavailability of neighbor information, which is equivalent to a crash. However, switching topologies will provide a compensatory means for the escalation of fault severity, and the FRFTC itself accommodates topology switching, and thus is an effective fault-tolerant algorithm for communication faults. As shown in Fig. 14, a scenario when UAV 4 is injected with a failure fault at $t = 20$ s and the entire UAV formation is greatly affected and deviates significantly due to the presence of network connectivity. Whereas, as the failure is actively interrupted in time at $t = 25$ s, and the formation returns stability.

In summary, it can be concluded that the proposed FRFTC algorithm can effectively suppress the interference caused by different fault types, but whether it can be received or not

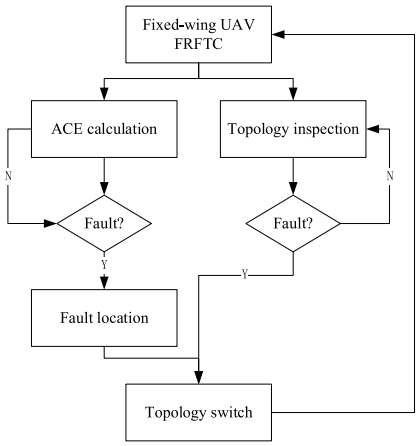

FIGURE 15. Formation security realization schema of fixed-wing UAV FRFTC.

depends on the required cooperative performance in practice. For example, for general reconnaissance missions, the relative position of the UAV is strictly required, the evaluation of the UAV performance would reach a more stringent level. For other tracking missions, the evaluation of the UAV performance would be more lenient. However, when the quantity of failure types increases, the algorithm's capability and robustness would decrease, which could be addressed by communication topology switch. The whole process as a formation security realization schema is illustrated in Fig. 15. In this schema, ACE provides an evaluation of formation performance be setting thresholds to determine whether or not topology should switch to avoid severe loss, which is practical in different fixed-wing UAV formations.

V. CONCLUSION

In this study, the challenges arising from the application of fixed-wing UAV formation, such as actuator faults of varying severity and communication disruptions, are systematically approached as a fault-tolerant control problem under switching topologies, ultimately leading to the proposal of an innovative formation robust fault-tolerant control method. Through the analysis of the consensus control method's structure, the study transforms the fixed-wing UAV formation control problem into an equivalent single transformation UAV system, where the eigenvalues of the Laplacian matrix of formation network serve as an amplification of a single entity. Building upon this groundwork, an advanced formation robust fault-tolerant control method is developed to effectively manage actuator faults swith switching topologies, treating faults and saturation as a form of disturbance. The proposed algorithm's feasibility is verified through comprehensive comparative analyses, which leads to a kind of formation security schema and provides an application scenario of the proposed method. It is expected that the work in this paper would be helpful to researchers with concerns like the formation security of cost-constrained fixed-wing UAVs.

In preparation for future application, complexity of the environment, nonlinearity of fixed-wing UAV system, diversity of fault types and varieties of switching strategies hold promising research significance and prospects. Developments on verification in hardware systems and high-level function with enough formation cooperative performance could be further proposed, like scouting, orienting and so on.

ACKNOWLEDGMENT

The authors would like to thank the editors and the reviewers for their efforts and hard work.

REFERENCES

[1] E. Soria, "Swarms of flying robots in unknown environments," *Sci. Robot.*, vol. 7, no. 66, May 2022, Art. no. eabq2215.
[2] H. Chen, X. Wang, L. Shen, and Y. Cong, "Formation flight of fixed-wing UAV swarms: A group-based hierarchical approach," *Chin. J. Aeronaut.*, vol. 34, no. 2, pp. 504–515, Feb. 2021.
[3] K. Cengiz, S. Lipsa, R. K. Dash, N. Ivković, and M. Konecki, "A novel intrusion detection system based on artificial neural network and genetic algorithm with a new dimensionality reduction technique for UAV communication," *IEEE Access*, vol. 12, pp. 4925–4937, 2024.
[4] K.-K. Oh, M.-C. Park, and H.-S. Ahn, "A survey of multi-agent formation control," *Automatica*, vol. 53, pp. 424–440, Mar. 2015.
[5] Y. Shi, J. Yu, Y. Hua, X. Dong, and Z. Ren, "Distributed formation flight for fixed-wing UAVs based on cooperative moving path following under wind disturbances," in *Proc. China Autom. Congr. (CAC)*, Oct. 2021, pp. 3114–3119.
[6] Z. Yu, Y. Zhang, B. Jiang, J. Fu, and Y. Jin, "A review on fault-tolerant cooperative control of multiple unmanned aerial vehicles," *Chin. J. Aeronaut.*, vol. 35, no. 1, pp. 1–18, Jan. 2022.
[7] X. Dong, B. Yu, Z. Shi, and Y. Zhong, "Time-varying formation control for unmanned aerial vehicles: Theories and applications," *IEEE Trans. Control Syst. Technol.*, vol. 23, no. 1, pp. 340–348, Jan. 2015.
[8] Y. Hua, X. Dong, J. Wang, Q. Li, and Z. Ren, "Time-varying output formation tracking of heterogeneous linear multi-agent systems with multiple leaders and switching topologies," *J. Franklin Inst.*, vol. 356, no. 1, pp. 539–560, Jan. 2019.
[9] C. Peng and F. Li, "A survey on recent advances in event-triggered communication and control," *Inf. Sci.*, vols. 457–458, pp. 113–125, Aug. 2018.
[10] Z. Yan, L. Han, X. Li, X. Dong, Q. Li, and Z. Ren, "Event-triggered formation control for time-delayed discrete-time multi-agent system applied to multi-UAV formation flying," *J. Franklin Inst.*, vol. 360, no. 5, pp. 3677–3699, Mar. 2023.
[11] C. Gao, X. He, H. Dong, H. Liu, and G. Lyu, "A survey on fault-tolerant consensus control of multi-agent systems: Trends, methodologies and prospects," *Int. J. Syst. Sci.*, vol. 53, no. 13, pp. 2800–2813, Oct. 2022.
[12] G. Wang, H. Luo, X. Hu, H. Ma, and S. Yang, "Fault-tolerant communication topology management based on minimum cost arborescence for leader–follower UAV formation under communication faults," *Int. J. Adv. Robotic Syst.*, vol. 14, no. 2, Mar. 2017, Art. no. 172988141769396.
[13] W. Cao, J. Zhang, and W. Ren, "Leader–follower consensus of linear multi-agent systems with unknown external disturbances," *Syst. Control Lett.*, vol. 82, pp. 64–70, Aug. 2015.
[14] S. Liang, S. Zhang, Y. Huang, X. Zheng, J. Cheng, and S. Wu, "Data-driven fault diagnosis of FW-UAVs with consideration of multiple operation conditions," *ISA Trans.*, vol. 126, pp. 472–485, Jul. 2022.
[15] R. Deng, J. Chen, M. Wang, Z. Shi, and Y. Zhong, "Fault detection and isolation for a fixed-wing UAV swarm system with uncertainties and disturbances," in *Proc. Chin. Control Conf. (CCC)*, Jul. 2019, pp. 4919–4924.
[16] C. Gao and X. He, "Fault-tolerant consensus control for multi-agent systems with actuator saturation," in *Proc. 33rd Youth Academic Annu. Conf. Chin. Assoc. Autom. (YAC)*, May 2018, pp. 484–488.
[17] Y. Liu, X. Dong, P. Shi, Z. Ren, and J. Liu, "Distributed fault-tolerant formation tracking control for multiagent systems with multiple leaders and constrained actuators," *IEEE Trans. Cybern.*, vol. 53, no. 6, pp. 3738–3747, Jun. 2023.

[18] Y. Yu, C. Guo, and T. Li, "Path following of underactuated autonomous surface vessels with surge velocity constraint and asymmetric saturation," *IEEE/CAA J. Autom. Sinica*, vol. 10, no. 5, pp. 1343–1345, May 2023.

[19] C. Hajiyev and H. E. Soken, "Robust adaptive Kalman filter for estimation of UAV dynamics in the presence of sensor/actuator faults," *Aerosp. Sci. Technol.*, vol. 28, no. 1, pp. 376–383, Jul. 2013.

[20] Y. Wu, Z. Wang, S. Ding, and H. Zhang, "Leader–follower consensus of multi-agent systems in directed networks with actuator faults," *Neurocomputing*, vol. 275, pp. 1177–1185, Jan. 2018.

[21] J. Chen, Z. Shi, and Y. Zhong, "Robust output formation control for uncertain multi-agent systems," *Int. J. Syst. Sci.*, vol. 51, no. 13, pp. 2456–2470, Oct. 2020.

[22] P. Yang, B. Ma, Y. Dong, and J. Liu, "Fault-tolerant consensus of leader-following multi-agent systems based on distributed fault estimation observer," *Int. J. Control, Autom. Syst.*, vol. 16, no. 5, pp. 2354–2362, Oct. 2018.

[23] J.-T. shi, X. He, and D.-H. Zhou, "Cooperative fault tolerant control for multi-vehicle systems," *J. Shanghai Jiaotong Univ.*, vol. 49, no. 6, pp. 819–824, 2015.

[24] Y. Xu and Z.-G. Wu, "Distributed adaptive event-triggered fault-tolerant synchronization for multiagent systems," *IEEE Trans. Ind. Electron.*, vol. 68, no. 2, pp. 1537–1547, Feb. 2021.

[25] G. Zhang, J. Qin, W. X. Zheng, and Y. Kang, "Fault-tolerant coordination control for second-order multi-agent systems with partial actuator effectiveness," *Inf. Sci.*, vol. 423, pp. 115–127, Jan. 2018.

[26] B. Zhang, X. Sun, S. Liu, M. Lv, and X. Deng, "Event-triggered adaptive fault-tolerant synchronization tracking control for multiple 6-DOF fixed-wing UAVs," *IEEE Trans. Veh. Technol.*, vol. 71, no. 1, pp. 148–161, Jan. 2022.

[27] Z. Yu, Y. Zhang, B. Jiang, C.-Y. Su, J. Fu, Y. Jin, and T. Chai, "Refined fractional-order fault-tolerant coordinated tracking control of networked fixed-wing UAVs against faults and communication delays via double recurrent perturbation FNNs," *IEEE Trans. Cybern.*, vol. 54, no. 2, pp. 1189–1201, Feb. 2024.

[28] Z. Yu, J. Li, Y. Xu, Y. Zhang, B. Jiang, and C.-Y. Su, "Reinforcement learning-based fractional-order adaptive fault-tolerant formation control of networked fixed-wing UAVs with prescribed performance," *IEEE Trans. Neural Netw. Learn. Syst.*, vol. 35, no. 3, pp. 3365–3379, Mar. 2024.

[29] B. Qin, D. Zhang, S. Tang, and Y. Xu, "Two-layer formation-containment fault-tolerant control of fixed-wing UAV swarm for dynamic target tracking," *J. Syst. Eng. Electron.*, vol. 34, no. 6, pp. 1375–1396, Dec. 2023.

[30] Z.-G. Wu, Y. Xu, R. Lu, Y. Wu, and T. Huang, "Event-triggered control for consensus of multiagent systems with fixed/switching topologies," *IEEE Trans. Syst. Man, Cybern. Syst.*, vol. 48, no. 10, pp. 1736–1746, Oct. 2018.

[31] W. Xu, D. W. C. Ho, L. Li, and J. Cao, "Event-triggered schemes on leader-following consensus of general linear multiagent systems under different topologies," *IEEE Trans. Cybern.*, vol. 47, no. 1, pp. 212–223, Jan. 2017.

[32] S. Zhou, X. Wei, X. Dong, Y. Hua, and Z. Ren, "Time-varying group formation-tracking control for heterogeneous multi-agent systems with switching topologies and time-varying delays," in *Proc. 40th Chin. Control Conf. (CCC)*, Jul. 2021, pp. 194–199.

[33] P. Shu, Y. Hua, X. Dong, and Z. Ren, "Distributed time-varying formation optimal tracking for multi-agent systems with optimal formation reference," in *Proc. IEEE Int. Conf. Unmanned Syst. (ICUS)*, Oct. 2021, pp. 548–553.

[34] H. Cheng, R. Song, L. Xu, D. Zhang, and S. Xu, "H_∞ consensus design and online scheduling for multiagent systems with switching topologies via deep reinforcement learning," *Int. J. Aerosp. Eng.*, vol. 2022, pp. 1–15, Mar. 2022.

[35] S. Huang, R. S. H. Teo, J. L. P. Kwan, W. Liu, and S. M. Dymkou, "Distributed UAV loss detection and auto-replacement protocol with guaranteed properties," *J. Intell. Robotic Syst.*, vol. 93, nos. 1–2, pp. 303–316, Feb. 2019.

[36] X. Wang, "Distributed formation output regulation of switching heterogeneous multi-agent systems," *Int. J. Syst. Sci.*, vol. 44, no. 11, pp. 2004–2014, Nov. 2013.

[37] Q. Wang, Y. Hua, X. Dong, P. Shu, J. Lü, and Z. Ren, "Finite-time time-varying formation tracking for heterogeneous nonlinear multiagent systems using adaptive output regulation," *IEEE Trans. Cybern.*, early access, Mar. 12, 2023, doi: 10.1109/TCYB.2023.3245139.

[38] H. Yang, B. Jiang, H. Yang, and H. H. T. Liu, "Fault-tolerant cooperative control for multiple vehicle systems based on topology reconfiguration," *IEEE Trans. Cybern.*, vol. 52, no. 7, pp. 6649–6661, Jul. 2022.

[39] K.-Z. Miao, J.-N. Li, Y.-J. Chen, and S. Xu, "Finite-time fault-tolerant consensus for leader-following multi-agent systems with semi-Markov switching topologies," *Int. J. Control*, vol. 97, no. 2, pp. 373–386, Nov. 2022.

[40] X. Wu, Z. Guo, X. Liu, and T. Xie, "Fault-tolerant time-varying formation tracking control for multi-agent systems with actuator faults and switching topologies," *IEEE Access*, vol. 11, pp. 131140–131151, 2023.

[41] P. Kumar, S. K. Sonkar, R. C. George, D. Philip, and A. K. Ghosh, "Data-driven approach for estimating longitudinal aerodynamic parameters using neural artificial bee colony fusion algorithm," *Asian J. Control*, pp. 1–23, Jul. 2023, doi: 10.1002/asjc.3164.

[42] S. X. Ding, *Model-Based Fault Diagnosis Techniques-Design Schemes, Algorithms and Tools*. New York, NY, USA: Springer, 2013.

[43] J. Huang, *Nonlinear Output Regulation: Theory and Applications*. Philadelphia, PA, USA: SIAM, 2004.

[44] H. Zhang, L. Dou, B. Xin, J. Chen, M. Gan, and Y. Ding, "Data collection task planning of a fixed-wing unmanned aerial vehicle in forest fire monitoring," *IEEE Access*, vol. 9, pp. 109847–109864, 2021.

[45] W. Liu, H. Dai, S. Yan, Y. Qi, and X. Wu, "Dynamic H_∞ consensus of higher-order nonlinear multi-agent systems with general directed topology," *IEEE Access*, vol. 10, pp. 21316–21326, 2022.

JINLIN LI received the B.S. degree in mechanical engineering from Tsinghua University, Beijing, China, in 2021, where he is currently pursuing the master's degree with the Department of Mechanical Engineering. His current research interests include fixed-wing UAV design, formation control, and fault diagnosis.

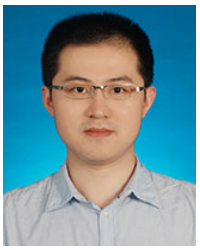

FEI GUO received the B.S. degree in mechanical engineering from Harbin Institute of Technology (HIT), Harbin, China, in 2010, and the Ph.D. degree in mechanical engineering from Tsinghua University, Beijing, China, in 2014.

He is currently an Associate Professor with the Department of Mechanical Engineering, Tsinghua University. His current research interests include rubber and plastic seals, special static sealing technology, and intelligent algorithms. He was a recipient of the Gold Award for Exhibition of Inventions Geneva, the Second Prize for National Technological Invention Award, the First Prize for Guangdong Science and Technology Progress Award, the First Prize for China Machinery Industry Science and Technology Award, and the First Prize for Technological Invention Award of Ministry of Education.

JUNMIN ZHAO received the B.S. degree in detection and control technology from Northwestern Polytechnical University, Xi'an, China, in 2003, and the M.S. degree in detection guidance and control technology from Xi'an Institute of Modern Control Technology, Xi'an, in 2006. He is currently pursuing the Ph.D. degree in flight vehicle design with Northwestern Polytechnical University. His research interests include aircraft task planning, control system design, and the fixed-wing UAV overall design.